Ke et al. *Zool. Res.* 2024, 45(3): 633−647
https://doi.org/10.24272/j.issn.2095-8137.2023.412

ZR | Zoological Research

Article Open Access

Functional dissection of parabrachial substrates in processing nociceptive information

Jin Ke[1,2,3,#], Wei-Cheng Lu[4,#], Hai-Yang Jing[1,2,#], Shen Qian[1,2,5], Sun-Wook Moon[1,2], Guang-Fu Cui[1,2], Wei-Xin Qian[1,2,5], Xiao-Jing Che[1,2,3], Qian Zhang[6], Shi-Shi Lai[7], Ling Zhang[1,2], Ying-Jie Zhu[1,2,*], Jing-Dun Xie[4,*], Tian-Wen Huang[1,2,*]

[1] *Shenzhen Key Laboratory of Drug Addiction*, *Shenzhen-Hong Kong Institute of Brain Science*, *Brain Cognition and Brain Disease Institute*, *Shenzhen Institute of Advanced Technology*, *Chinese Academy of Sciences*, *Shenzhen*, *Guangdong* 518055, *China*

[2] *CAS Key Laboratory of Brain Connectome and Manipulation*, *Brain Cognition and Brain Disease Institute*, *Shenzhen Institute of Advanced Technology*, *Chinese Academy of Sciences*, *Shenzhen*, *Guangdong* 518055, *China*

[3] *University of Chinese Academy of Sciences*, *Beijing* 100049, *China*

[4] *Department of Anesthesiology*, *State Key Laboratory of Oncology in South China*, *Guangdong Provincial Clinical Research Center for Cancer*, *Sun Yat-sen University Cancer Center*, *Guangzhou*, *Guangdong* 510060, *China*

[5] *University of Science and Technology of China*, *Hefei*, *Anhui* 230027, *China*

[6] *Department of Anesthesiology*, *Shenzhen University General Hospital and Shenzhen University Academy of Clinical Medical Sciences*, *Shenzhen University*, *Shenzhen*, *Guangdong* 518055, *China*

[7] *School of Medicine*, *Yunnan University*, *Kunming*, *Yunnan* 650091, *China*

ABSTRACT

Painful stimuli elicit first-line reflexive defensive reactions and, in many cases, also evoke second-line recuperative behaviors, the latter of which reflects the sensing of tissue damage and the alleviation of suffering. The lateral parabrachial nucleus (lPBN), composed of external- (elPBN), dorsal- (dlPBN), and central/superior-subnuclei (jointly referred to as slPBN), receives sensory inputs from spinal projection neurons and plays important roles in processing affective information from external threats and body integrity disruption. However, the organizational rules of lPBN neurons that provoke diverse behaviors in response to different painful stimuli from cutaneous and deep tissues remain unclear. In this study, we used region-specific neuronal depletion or silencing approaches combined with a battery of behavioral assays to show that slPBN neurons expressing substance P receptor (*NK1R*) ($lPBN^{NK1R}$) are crucial for driving pain-associated self-care behaviors evoked by sustained noxious thermal and mechanical stimuli applied to skin or bone/muscle, while elPBN neurons are dispensable for driving such reactions. Notably, $lPBN^{NK1R}$ neurons are specifically required for forming sustained somatic pain-induced negative teaching signals and aversive memory but are not necessary for fear-learning or escape behaviors elicited by external threats. Lastly, both $lPBN^{NK1R}$ and elPBN neurons contribute to chemical irritant-induced nocifensive reactions. Our results reveal the functional organization of parabrachial substrates that drive distinct behavioral outcomes in response to sustained pain versus external danger under physiological conditions.

Keywords: Lateral parabrachial nucleus; Substance P receptor; Pain affect; Defensive reaction; Somatosensory

INTRODUCTION

Noxious stimuli are detected by primary sensory neurons, which innervate both cutaneous (primarily the skin epidermis) and deep tissues (including muscle, bone, and visceral organs) throughout the body (Huang et al., 2019; Yang et al., 2013; Zylka et al., 2005). These stimuli elicit two sets of behaviors. The first includes reflexive defensive reactions, such as rapid withdrawal or jumping from a hot plate, reflecting the sensing of external threats (exteroception) and serving as first-line protective responses to prevent or limit tissue damage. When these first-line reactions fail to protect the body, second-line recuperative behaviors are invoked, which involve the sensing of any disruption of body integrity (interoception, not only for visceral sensation but also

Received: 18 April 2024; Accepted: 11 May 2024; Online: 12 May 2024

Foundation items: This work was supported by the Shenzhen Key Laboratory of Drug Addiction (ZDSYS20190902093601675), CAS Key Laboratory of Brain Connectome and Manipulation (2019DP173024), National Natural Science Foundation of China (82274358), Shenzhen-Hong Kong Institute of Brain Science, and Guangdong Basic and Applied Basic Research Foundation (2023B1515040009)

[#]Authors contributed equally to this work

*Corresponding authors, E-mail: yj.zhu1@siat.ac.cn; xiejd6@mail.sysu.edu.cn; tw.huang@siat.ac.cn

including skin damage), including persistent licking of injured body parts to alleviate suffering ("self-care") (Chen et al., 2021; Huang et al., 2019; Ma, 2022). The long-standing debate regarding which behaviors reliably reflect the sensory and emotional experience of pain in animals (Cobos & Portillo-Salido, 2013; Mogil, 2009; Sluka, 2013) has led to calls for reevaluating the widespread use of reflexive defensive reactions as surrogate measures for clinically relevant tonic pain (Beecher, 1957; Ma, 2022; Mao, 2012; Mogil, 2018; Tappe-Theodor et al., 2019).

Research suggests that, under physiological conditions, the somatosensory system contains functional subdivisions for exteroception and interoception, which drive the two sets of behaviors described above (Han et al., 2015; Head, 1911; Huang et al., 2019; Ma, 2022; Mark et al., 1960, 1963). Our previous research demonstrated that, at the spinal level, dorsal horn neurons expressing the preprotachykinin1 gene (*Tac1*, which encodes neuropeptide substance P) are required for driving interoceptive self-care behaviors associated with sustained pain derived from the skin but are not needed for immediate reflexive defensive reactions to external threats, with this functional segregation also applicable to primary sensory neurons (Huang et al., 2019; Ma, 2022). Anatomically, dorsal horn *Tac1*$^+$ neurons form a subset of spinal projection neurons that predominantly send axons to the most dorsal region of the lateral parabrachial nucleus (lPBN) (Barik et al., 2021; Choi et al., 2020; Huang et al., 2019), spurring considerable interest in the identification of lPBN neurons that act as downstream targets of spinal *Tac1*$^+$ projection neurons, which are essential for driving behaviors associated with sustained pain.

The lPBN serves as a crucial relay station in ascending pathways, receiving dense innervations from spinal projection neurons (Barik et al., 2018, 2021; Campos et al., 2018; Chiang et al., 2020; Choi et al., 2020; Deng et al., 2020; Huang et al., 2019; Ma, 2022). lPBN neurons respond to a variety of sensory inputs from almost all body regions and contribute to the emotional, autonomic, and neuroendocrine aspects of pain (Buritova et al., 1998; Campos et al., 2018; Gauriau & Bernard, 2002; Huang et al., 2019; Menendez et al., 1996; Palmiter, 2018; Rodella et al., 1998). According to the Allen Brain Atlas, the lPBN is divided into several subnuclei: the superior-central lPBN (slPBN, the most dorsal part), external lPBN (elPBN, the most ventral part), and dorsal lPBN (dlPBN, the intermedial part between the slPBN and elPBN) (Chiang et al., 2019; Choi et al., 2020; Fulwiler & Saper, 1984; Hashimoto et al., 2009; Huang et al., 2019). These sub-nuclei are identified by specific neuronal subtypes and relay sensory information to the central amygdala, medial thalamic complex, and other brain regions to generate diverse behavioral, autonomic, and emotional responses (Barik et al., 2018; Chiang et al., 2020; Huang et al., 2021a, 2021b; Jaramillo et al., 2021; Kim et al., 2013; Ma, 2022; Palmiter, 2018; Pauli et al., 2022; Saper, 2016; Sun et al., 2020; Tovote et al., 2015). Calcitonin-related polypeptide (*Calca*)-positive neurons, enriched in the elPBN, are activated by noxious cutaneous and visceral stimuli, and are required for appetitive and fear-associated responses, as well as rapid defensive reactions to electric foot shocks and escape behaviors in response to hot plate exposure (Campos et al., 2018; Han et al., 2015; Palmiter, 2018). In addition to *CGRP*$^+$ elPBN neurons, *Tac1*$^+$ neurons located in the elPBN modulate escape responses via the brainstem-spinal descending pathway (Barik et al., 2018; Roeder et al., 2016). In contrast, dlPBN neurons relay thermal information and are involved in behavioral thermoregulation (Yahiro et al., 2017), with dlPBN *Pdyn*$^+$ neurons found to convey nociceptive information from the spinal cord to the elPBN via a local circuit within the lPBN (Chiang et al., 2020). Substance P receptor (*NK1R*)-expressing neurons (lPBN^{NK1R}) enriched in the slPBN respond to noxious thermal, mechanical, and electric foot shock stimuli, and are required for driving licking behaviors elicited by formalin injection (Barik et al., 2021; Choi et al., 2020; Deng et al., 2020; Roeder et al., 2016). However, the overall functional organization of lPBN subdivisions in driving distinct behaviors elicited by sustained pain from cutaneous and deep tissues under physiological conditions remains unclear.

In this study, using region-specific neuronal ablation and silencing approaches, combined with comprehensive screening of a series of behavioral assays, we investigated the function of elPBN and slPBN neurons in processing sustained pain and fear under physiological conditions. Results showed that lPBN^{NK1R} neurons are required for sustained somatic thermal and mechanical pain but are not necessary for fear-induced freezing behavior and aversive memory or escape responses to external threats. We also confirmed that elPBN neurons are essential for provoking defensive reactions to external threats but are dispensable for recuperative behaviors under sustained somatic thermal and mechanical pain. Lastly, we found both lPBN^{NK1R} and elPBN neurons are required for producing inflammatory irritant injection-evoked nocifensive behaviors.

MATERIALS AND METHODS

Animals

All procedures were performed in accordance with the guidelines established by the Chinese Council on Animal Care as approved by the Animal Care Committee of the Shenzhen Institute of Advanced Technology, Chinese Academy of Sciences (approval No. SIAT-IACUC-200319-NS-HTW-A1166). Mice were housed in a temperature-controlled room (22–25°C) under 12 h light/dark cycle and were provided with standard laboratory mouse pellet food and *ad libitum* access to water. Male and female *C57BL/6J* and *NK1R-CreGFP* mice (8–10 weeks old) were used for all experiments. The *C57BL/6J* mice were purchased from the Charles River Laboratory. The *NK1R-CreGFP* mice were generated and kindly provided by Dr. Xinzhong Dong at Johns Hopkins University (Xu et al., 2021). Both male and female mice were randomly assigned to different treatment groups.

The *NK1R-CreGFP* mice were crossed with wild-type *C57BL/6J* mice to produce F1 progenies. The genotypes were identified by polymerase chain reaction (PCR) analysis of tail-snip DNA using loci-specific primers targeting the junction between *NK1R* and *Cre* genes, and the junction between *EGFP* and 3'UTR of *NK1R*: Forward primer: 5'-TATCTC ACGTACTGACGGTG-3'; Reverse primer: 5'-CTAATCGCCA TCTTCCAGC-3'.

Viruses and chemical reagents

The following viral tools were used: AAV9-hSyn-DIO-mCherry (BC-0025), AAV9-hSyn-DIO-hM4D(Gi)-mCherry (BC-0153), AAV9-hSyn-DIO-taCasp3-TEVp (BC-0128), AAV9-hSyn-DIO-EGFP (BC-0244), and AAV9-hSyn-DIO-GCaMP6s (BC-0238), all of which were obtained from BrainCase (China). Ibotenic

acid (IBO) was purchased from APExBIO (No. B6246, USA). The *NK1R*, *vGlut2*, and *VGAT* mRNA probes were designed by Spatial FISH (China). Clozapine-N-oxide (No. C0832) and acetic acid (No. 695092) were purchased from Sigma (USA). The following primary and secondary antibodies were used in this study: mouse anti-NeuN (1:500, Sigma, MAB377, USA), rabbit anti-c-Fos (1:500, Abcam, ab190289, USA), chicken anti-GFP (1:500, Abcam, ab13970, USA), rabbit anti-mCherry (1:500, Abcam, ab167453, USA), goat anti-rabbit 488 (1:200, Jackson ImmunoResearch Laboratories, 111-545-003, USA), donkey anti-mouse 594 (1:200, Jackson ImmunoResearch Laboratories, 715-587-003, USA), goat anti-rabbit 594 (1:200, Jackson ImmunoResearch Laboratories, 111-585-003, USA), goat anti-chicken 488 (1:200, Jackson ImmunoResearch Laboratories, 103-547-008, USA), and 4',6-diamidino-2-phenylindole (DAPI, 1:5 000; Sigma, D9542, USA).

Stereotaxic and viral injection surgery

The animals underwent isoflurane anesthesia (3% for induction and 1.4% for maintenance; maintained under 100% O_2) and were placed in a stereotaxic head frame (RWD Life Science, China). The scalp was shaved, and a local antiseptic (Betadine, Sigma, USA) was applied. A midline incision was made to expose the cranium, which was then carefully drilled with a micromotor handpiece drill (Foredom, USA). Two holes were drilled for stereotaxic viral injection. The AAV vectors were stereotaxically injected with a glass pipette connected to a Nanoliter Injector (Drummond Scientific Company, USA) at a slow flow rate of 60 nL/min to avoid potential damage to local brain tissue. The pipette was withdrawn at least 10 min after the viral injection. The virus was injected unilaterally or bilaterally into the lPBN: antero-posterior (AP) –5.30 mm, mediolateral (ML) ±1.35 mm, dorsoventral (DV) –3.40 mm, slPBN: antero-posterior (AP) –5.25 mm, mediolateral (ML) ±1.30 mm, dorsoventral (DV) –3.25 mm, and elPBN: antero-posterior (AP) –5.30 mm, mediolateral (ML) ±1.45 mm, dorsoventral (DV) –3.70 mm from the skull surface. All viruses were injected at a volume of 200–300 nL/site.

To manipulate lPBN^{NK1R} neuronal activity, AAV9-hSyn-DIO-hM4D(Gi)-mCherry virus was bilaterally injected into the lPBN of *NK1R-CreGFP* mice, while AAV9-hSyn-DIO-mCherry virus was injected as a control.

To ablate lPBN^{NK1R} neurons, AAV9-hSyn-DIO-taCasp3-TEVp virus was bilaterally injected into the lPBN of *NK1R-CreGFP* mice, while AAV9-hSyn-DIO-mCherry-TEVp virus was injected as a control.

To ablate lPBN and elPBN neurons, 300 nL (for lPBN) or 150 nL (for elPBN) of IBO (5 mmol/L) was bilaterally injected into the *C57BL/6J* mice, while saline was injected as a control.

To examine the response of lPBN^{NK1R} neurons to painful stimuli, AAV9-hSyn-DIO-GCaMP6s virus was injected into the lPBN, while AAV9-hSyn-DIO-EGFP virus was injected as a control. An optical fiber (200 μm in diameter, 0.37 NA, 5 mm in length, ThinkerTech, China) was subsequently implanted 150 μm above the viral injection site and affixed with a skull-penetrating screw and dental acrylic.

Immunohistochemistry and fluorescent *in situ* hybridization

Mice were intraperitoneally injected with sodium pentobarbital (80 mg/kg), then transcardially perfused with 20 mL of ice-cold phosphate-buffered saline (PBS, pH=7.4), followed by 20 mL of 4% paraformaldehyde (PFA, Sigma, USA). After perfusion, the tissues were dissected and post-fixed in 4% PFA overnight at 4°C, followed by dehydration in 25% sucrose solution. The samples were then frozen in OCT at −20°C, after which transverse sections (40 μm) were sliced using a cryostat microtome (Leica CM1950, Leica, Germany) and immediately subjected to histochemical staining. Immunofluorescent staining was performed as described previously (Huang et al., 2019). In brief, tissue sections were washed in 0.01 mol/L PBS for 15 min and treated with blocking solution (5% normal donkey serum and 0.3% Triton X-100 in 0.01 mol/L PBS) at room temperature for 1 h, then incubated with primary antibodies diluted in blocking solution overnight at 4°C. After washing three times in 0.01 mol/L PBS for 10 min, the sections were incubated for 2 h at room temperature with a secondary antibody. Finally, sections were washed in 0.01 mol/L PBS three times for 10 min, stained with DAPI for 10 min, and mounted. Fluorescent *in situ* hybridization was performed on brain sections as described previously (Han et al., 2023). Specific probes for target genes were designed by Spatial FISH (China), including vesicular glutamate transporter 2 (*vGlut2/Slc17a6*, NM_009508.1), vesicular GABA transporter (*VGAT/Slc32a1*, NM_009508.1), and substance P receptor (*NK1R/Tacr1*, NM_009313.3). Samples were fixed with 4% PFA, then covered with a reaction chamber to perform the following reactions: After dehydration and denaturation with methanol, the samples were incubated at 37°C overnight with a hybridization buffer containing specific target probes. Subsequently, the samples were washed three times with PBST, followed by 3 h of incubation at 25°C with the target probes mixed in the ligation solution. After another three washes with PBST, the samples underwent overnight incubation at 30°C for rolling circle amplification with Phi29 DNA polymerase. Next, fluorescent detection probes in the hybridization buffer were applied to the sample. Finally, the samples were dehydrated using an ethanol series and mounted with a mounting medium. Images are captured, and signal spots were decoded to interpret the RNA spatial location information.

Electrophysiological recordings

Acute brain slice preparation and whole-cell patch recordings were performed as described previously (Hou et al., 2023; Hu et al., 2022). Briefly, 3 weeks after AAV9-hSyn-DIO-hM4D(Gi)-mCherry viral injection, the *NK1R-CreGFP* mice were anesthetized with isoflurane and decapitated. Brains were rapidly dissected, and coronal slices (300 μm) containing the lPBN were prepared using a vibratome (VT-1000S, Leica, Germany) in an ice-cold choline-based solution containing the following reagents (in mmol/L): 110 choline chloride, 2.5 KCl, 0.5 $CaCl_2$, 7 $MgCl_2$, 1.3 NaH_2PO_4, 1.3 Na-ascorbate, 0.6 Na-pyruvate, 25 glucose, and 25 $NaHCO_3$, saturated with 95% O_2 and 5% CO_2. Slices were incubated in 36°C oxygenated artificial cerebrospinal fluid (aCSF) containing the following reagents (in mmol/L): 125 NaCl, 2.5 KCl, 2 $CaCl_2$, 1.3 $MgCl_2$, 1.3 NaH_2PO_4, 1.3 Na-ascorbate, 0.6 Na-pyruvate, 25 glucose, and 25 $NaHCO_3$, for at least 1 h before recording. Slices were transferred to a recording chamber and superfused with aCSF at 2 mL/min. Patch pipettes (3–6 MΩ) were made of borosilicate glass (#BF150-86-10, Sutter Instruments, USA). For action potential firing recordings, the pipettes were filled with K^+-based internal solution containing the following reagents (in mmol/L): 130 K-gluconate, 10 KCl, 10 HEPES, 1 EGTA, 2 Mg-ATP, 0.3 Na-GTP, 2 $MgCl_2$, 290 mOsm/kg, adjusted to pH 7.3 with potassium hydroxide. To measure the

inhibitory effects of CNO treatment, hM4Di-mCherry-expressing lPBN^{NK1R} neurons were injected with a 50 pA current, and the number of action potentials was calculated as the baseline. Subsequently, 10 μmol/L CNO was applied to the brain slices by bath perfusion, and the action potentials induced by 50 pA current injections were recorded. Whole-cell voltage-clamp recordings were performed at room temperature (22–25°C) using a MultiClamp 700B amplifier and Digidata 1550B system (Molecular Devices, USA). Data were sampled at 10 kHz and analyzed using pClamp10 (Molecular Devices, USA).

Behavioral tests

Following viral injection and optical fiber implantation, mice were allowed a minimum of 3 weeks for recovery before the behavioral tests. For lPBN- and elPBN-ablation experiments, the behavioral tests were performed 7 days after IBO injections. For the lPBN^{NK1R}-neuronal silencing experiment, the behavioral measurements began 30 min after intraperitoneal injection of CNO (3 mg/kg). We used the same sets of control and experimental groups of mice for all acute nociceptive behavioral tests (tests 1–9 in Figure 1A) in the lPBN-lesion, lPBN^{NK1R}-ablation/silencing, and elPBN-lesion experiments. For all conditioned place aversion tests, another group of control and experimental mice was used.

Mice were habituated for 30 min every day for 3 consecutive days before the behavioral tests. All behavioral experiments were conducted by experimenters blind to the genotypes and treatments of the mice and strictly followed the timeline as indicated in Figure 1A. To minimize tissue damage, the threshold-based tests for reflexive defensive behaviors were performed on the first and second days, followed by the hot plate, skin pinch, toe clip, and writhing tests at one day intervals, respectively. For the rotarod, von Frey, brush, and radiant heat tests performed on the same day, the interval between was 2 h. The rotarod, light touch (brush), radiant heat, cold plantar (dry ice), hot plate, von Frey, and skin pinch assays were performed as described previously (Bourane et al., 2015; Brenner et al., 2012; Cheng et al., 2017; Duan et al., 2014; Huang et al., 2019; Lou et al., 2013).

For the rotarod test, an accelerating rotarod was used to measure gross motor ability and coordination. Mice were trained on the rotarod for 3 min at a constant speed of 4 r/min, then tested by acceleration of the ramp from 0 to 40 r/min. Each mouse was subjected to three trials, with an interval of 10 min between each trial, and the latency to falling from the rod was calculated as the average of three trials.

For the brush test, mice were placed in a plastic chamber on an elevated wire grid and the plantar surface of the hind paw was lightly stimulated with a soft paintbrush from heel to toe. The average score of each mouse across three trials (3 min interval) was reported as the dynamic score (score 0: walk away or occasional very brief paw lifting; score 1: very short, fast-moving/raised claws; score 2: strong lateral lifting above the level of the body; score 3: flinching or persistent licking of affected hind paw).

For the radiant heat (Hargreaves') test (Hargreaves et al., 1988), mice were placed in a plastic chamber on a glass floor and a radiant heat beam (Ugo Basile, Italy) was applied to the hind paw. The latency for the animal to withdraw the hind paw was measured. Beam intensity was adjusted as control mice displayed a withdrawal latency of 5–15 s. A cutoff time of 30 s was used to avoid tissue damage. Each mouse was subjected to three trials, with 10 min intervals. The latency to paw withdrawal was defined as the average of all three trials.

For the hot plate test, mice were placed on a hot plate set to 50°C (Bioseb, France) and the latency of hind paw withdrawal and duration of hind paw licking were measured. Animals were tested sequentially with 5 min intervals. To avoid tissue injury, the cutoff time was set to 60 s.

For the cold plantar test, mice were acclimated to a glass plate (2 mm thick Pyrex borosilicate float glass) in transparent plastic enclosures (4 cm×4 cm×11 cm) separated by opaque black dividers for 1 h. Cylindrical dry ice was cut into 1 cm ports with a blade. Mice at rest but not asleep were tested by pressing the dry ice port onto the lower surface of the glass underneath the hind paw. Withdrawal latency was measured with a stopwatch and was defined as the animal moving its paw vertically or horizontally away from the cold glass area. Each mouse was subjected to three trials at 5 min intervals, with the average withdrawal latencies of the three trials then calculated.

For the von Frey test, mice were placed in a plastic chamber on wire mesh and the plantar surface of the hind paw was stimulated with a set of calibrated von Frey filaments (from 0.008 g to 2 g). The paw withdrawal threshold was determined according to Dixon's up-down method (Chaplan et al., 1994).

For the skin pinch test, an alligator clip (Amazon, Generic Micro Steel Toothless Alligator Test Clips 5AMP, USA) was applied to produce 340 g of force on the hind paw skin for 1 min, as described previously (Huang et al., 2019). The duration of licking the pinched area was calculated for each animal.

Toe clip tests, with or without lidocaine application, were performed as described in Supplementary Figure S1A. For toe clipping without lidocaine (toe clip w/o lidocaine), the same alligator clamp used in the skin pinch test was directly applied to the second phalanx of the middle toe for 1 min. This procedure activated both cutaneous and deep sensory fibers innervating the clipped toe area. To isolate deep tissue mechanical pain from the surrounding skin epidermis, lidocaine ointment (5%, Tongfang Pharmaceutical, China) was first applied to the entire hind paw skin, which was then wrapped with Parafilm for 15 min. The ointment was subsequently removed before the toe clipping assay. The duration of licking the clipped toe area was calculated for each animal. The blocking effect of lidocaine on superficial sensory fibers was confirmed by performing the skin pinch test on another set of animals using the same lidocaine application procedure on the hind paw skin. For simplification, "toe clip" stands for "toe clip w/ lidocaine" in the main figures and texts.

Acute peritoneovisceral pain was investigated using an acetic acid-induced writhing test. After intraperitoneal injection of acetic acid (0.6% in saline, 10 mg/kg), the mice were placed in transparent plastic boxes and the number of writhes was recorded for 30 min using a video camera. The writhing response was defined as abdominal muscle contractions, followed by stretching of the hindlimbs.

For the foot shock test, an electric shock was delivered by a stimulator (Jiliang, China) and an isolator (Model #3820, A-M Systems, USA). Animal behavior was automatically recorded and analyzed using the Any-maze® tracking system with default settings. In brief, after 3 consecutive days of habituation, each animal was allowed to freely explore the customized foot shock chamber for 5 min, followed by two

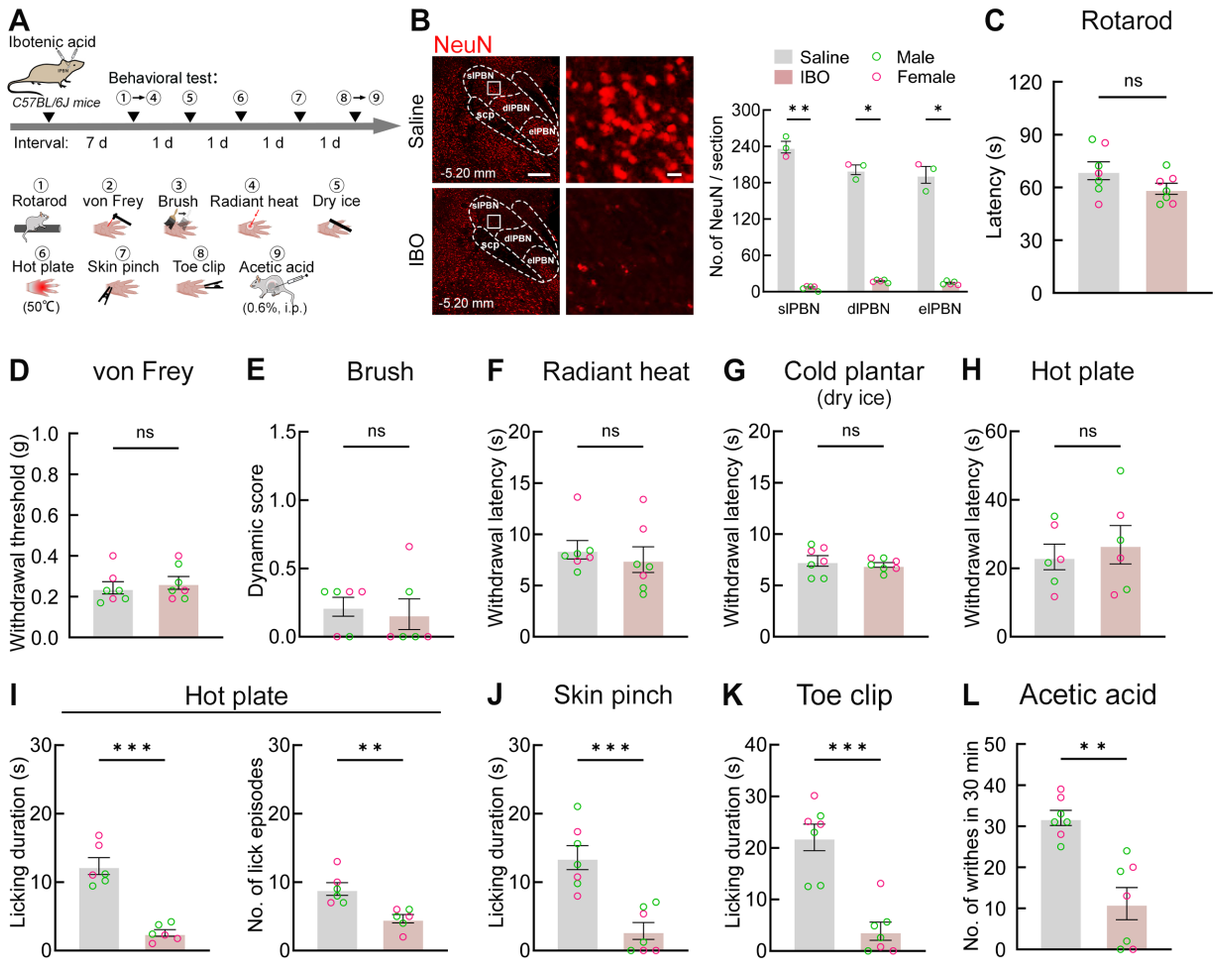

Figure 1 IPBN lesions affect sustained pain

A: Schematic of lPBN bilateral ibotenic acid (IBO) injection and behavioral paradigms. B: Left, representative immunostaining images of NeuN (red) in lPBN after saline control or IBO injection. Right, quantification of NeuN$^+$ cell number in slPBN, dlPBN, and elPBN subnuclei after IBO injection (n=3 mice in saline group, including two males and one female, n=5 mice in IBO group, including three males and two females, unpaired t-test for each lPBN subnucleus). Scale bars: 200 μm for lower magnification and 20 μm for boxed higher magnification, respectively. C: No detected differences were observed in falling latencies from the rotarod between the saline and IBO injection groups (n=7 mice per group, including four males and three females). D–H: Reflexive response tests. No significant differences were observed in withdrawal responses to von Frey filament (D), brush (E), radiant heat (F), dry ice (G), and hot plate (H) stimulation (n=6–7 mice, including 3–4 males and three females per group). I–K: lPBN-lesioned mice showed significantly reduced licking behaviors evoked by hot plate (I), skin pinching (J), and toe clipping (K) (n=6–7 mice, including 3–4 males and three females per group). L: lPBN-lesioned mice (n=7 mice per group, including four males and three females) showed reduced writhing behavior after acetic acid injection. Green and red circles represent male and female mice, respectively. Behavioral data are mean±SEM, unpaired t-test. ns: No significance; *: P<0.05; **: P<0.01; ***: P<0.001.

consecutive foot shocks (0.5 mA for 2 s with 2 min intervals). The mice were then returned to their home cages. After 24 h, the mice were taken to the shock-paired room for recall tests. Their behaviors immediately after and 24 h following electric foot shock conditioning were video-recorded, and freezing episodes were defined as a complete absence of movement other than breathing.

The conditioned place aversion (CPA) test was performed as described previously (Huang et al., 2019). In brief, the CPA chamber (30 cm length×30 cm width×20 cm height) consisted of two compartments: Compartment A featured a wall decorated with black and white grid patterns and a floor made of steel wires spaced 2 mm apart; Compartment B featured a wall decorated with black and white vertical strips (3 cm in width) and a floor made of iron wire mesh with 8 mm×8 mm lattice checks. During the habituation phase (Days 1–3), each mouse was gently handled three times over a 30 min period each afternoon. On training days (Days 5–8), in the morning session, each mouse in both the control and experimental groups was confined to Compartment A, and gently handled three times at 5 min intervals, without skin pinch or toe clip stimulation; in the afternoon session, each mouse in both the control and experimental groups was confined to Compartment B. The control animals were handled in the same way as in the morning, while the experimental mice were subjected to three trials of hind paw skin pinch or toe clip (1 min for each trial, 4 min intervals between trials). For baseline measurement and post-conditioning test days (Days 4 and 9), the mice were first confined for 1 min in a small chamber (30 cm length×5 cm width×20 cm height) between the two compartments. They were then allowed free access to both compartments for a total of 15 min, with behaviors and movements recorded using a video camera. The time spent by each mouse in each compartment was calculated using the

Any-maze® tracking system. Mice that spent more than 80% of the total time in one compartment during baseline measurement were excluded. The aversion score was calculated as the value of "post-conditioning duration minus baseline duration" that each mouse spent in the skin pinch- or toe clip-paired compartment.

Fiber photometry

For the fiber photometry test, Ca^{2+} signals were recorded using an F-scope (ThinkerTech, China) to measure $lPBN^{NK1R}$ neuronal activity in freely moving mice. To test neuronal activity in response to mechanical stimulation, each mouse underwent a single skin pinch or toe clip trial for 4 s using the same alligator clip as described above, brush stimulation for 2 s, or punctate mechanical stimulation by a 0.4 g von Frey filament for 2 s. To examine neuronal activity in response to thermal stimulation, the mice were placed on a 50°C hot plate for 6 s. For peritoneovisceral stimulation, Ca^{2+} signal changes were recorded for 10 min after intraperitoneal injection of acetic acid (0.6% in saline, 10 mL/kg). GCaMP6s fluorescent signals from $lPBN^{NK1R}$ neurons were obtained using fiber photometry (488 nm laser as the excitation light and 405 nm laser as the control light; Thinker Tech Nanjing Bioscience Inc, China). *ΔF/F* was calculated using Matlab 2021 software.

c-Fos induction

For skin pinch- or toe clip-evoked c-Fos expression, each mouse was housed alone for 3 days. The mice were subjected to gentle handling for 10 s, five times each day in their home cages to minimize the background level of c-Fos. On the test day, each mouse was habituated to the empty cage for 30 min, then subjected to hind paw skin pinch or toe clip (with or without lidocaine topical application) for 1 min. Perfusion was performed 90 min after each mechanical stimulation.

For acetic acid-evoked c-Fos expression, each mouse was habituated to the chamber for 30 min, then administered an intraperitoneal injection of acetic acid as described above. Perfusion was performed 120 min after injection.

For von Frey-evoked c-Fos expression, each mouse was placed in a plastic chamber on an elevated wire mesh, with the plantar surface of the hind paw then stimulated with a 0.4 g von Frey filament for 2 s. Each mouse was subjected to three trials of hind paw stimulation, with 10 s intervals. Perfusion was performed 90 min after the last stimulation.

For brush-evoked c-Fos expression, each mouse was placed in a plastic chamber on an elevated wire mesh, with the plantar surface of the hind paw then lightly brushed with a soft paintbrush from heel to toe. Each mouse was subjected to three trials (1 min/trial), with an interval of 1 min. Perfusion was performed 90 min after the last stimulation.

Imaging and data analysis

Images were taken using an Olympus VS-120 microscope, Olympus FV3000 confocal microscope (Japan), and Zeiss LSM 900 confocal microscope (Germany). Cell counting and image processing were carried out using Adobe Photoshop and Adobe Illustrator software. The lPBN was identified according to *The Mouse Brain in Stereotaxic Coordinates*, *Fourth Edition* (Paxinos & Franklin, 2013). For statistical analysis, average numbers from four different slices (bregma: –4.96 mm, –5.02 mm, –5.20 mm, and –5.34 mm) covering the whole lPBN from the rostral to caudal were calculated for each mouse.

To plot the distribution patterns of $NK1R^{GFP}$ neurons, lPBN- and elPBN-lesioned regions, and reagent injection and optical fiber implantation sites, the same series of rostral to caudal lPBN sections from 3–6 mice were aligned to the reference atlas, with locations manually marked and merged. To quantify the co-expression of *NK1R*, *vGlut2*, and *VGAT* mRNAs, we referenced the Allen Brain Cell Atlas dataset (Zhuang-ABCA-2 MERFISH whole brain coronal 2; https://portal.brain-map.org/atlases-and-data/bkp/abc-atlas). The co-expression from one representative lPBN slice at bregma −5.20 mm is shown (Yao et al., 2023).

Statistical analysis

All statistical analyses were performed using GraphPad Prism v.8.0. Normality of the datasets was assessed using the *t*-test, and if normality was not met, the Mann-Whitney rank-sum test was applied. Handle-, skin pinch with or without lidocaine-, and toe clip with or without lidocaine-induced c-Fos expression in the lPBN was assessed using one-way analysis of variance (ANOVA) followed by *post hoc* Holm-Sidak's test. For the foot shock-evoked freezing responses, data were assessed using two-way ANOVA followed by *post hoc* Bonferroni's test. The Chi-square test (two-tailed) was used to compare the percentage of mice in the control and experimental groups that exhibited jumping on the hot plate. Details on statistical methods are included in the figure legends. Results are presented as mean±standard error of the mean (SEM). *P*-values below or equal to 0.05 were considered statistically significant.

RESULTS

lPBN neurons are necessary for relaying sustained pain

As lPBN neurons respond to sensory information from both cutaneous and deep tissues and transmit to higher order centers (Basbaum et al., 2009; Gauriau & Bernard, 2002; Palmiter, 2018), we first confirmed the necessity of these neurons in cutaneous and deep pain-associated behavioral outcomes. To pharmacologically deplete lPBN neurons, IBO was bilaterally injected into the lPBN of *C57BL/6J* mice 7 days before the behavioral tests (Figure 1A). Immunostaining of the neuronal marker NeuN indicated almost complete neuronal loss in the lPBN following IBO injection (Figure 1B). In the behavioral tests, since clipping the toe without blocking the superficial sensory fibers by lidocaine will activate both cutaneous and deep tissue sensory fibers, we applied anesthetic lidocaine ointment over the entire hind paw to isolate deep tissue mechanical pain from the surrounding skin epidermis, and then performed the toe clip test (Supplementary Figure S1A). Results showed that topical application of lidocaine eliminated skin pinch-induced persistent licking (Supplementary Figure S1B) but did not affect such behavior induced by toe clipping (Supplementary Figure S1C). Consistent with the behavioral results, topical application of lidocaine significantly blocked the skin pinch-induced increase in the expression of the immediate early gene *c-Fos* (a marker of neuronal activation) in the slPBN but did not completely block the induction of *c-Fos* expression in toe-clipped mice (Supplementary Figure S1D–F). Although the number of $c\text{-}Fos^+$ neurons in the slPBN was reduced in the lidocaine-treated group compared to the no-lidocaine group, possibly reflecting the blockade of superficial sensory fibers by lidocaine, the remaining $c\text{-}Fos^+$ slPBN neurons, which were largely activated by deep tissue sensory fibers innervating the

clipped toe area, were still sufficient to drive a comparable level of sustained licking as the controls (Supplementary Figure S1C, D, F). Thus, further toe clip tests were conducted on mice with topical lidocaine application to the hind paw, serving as the behavioral model for investigating sustained deep tissue mechanical pain.

Ablation of lPBN neurons did not affect general sensorimotor coordination (Figure 1C) or withdrawal responses to punctate mechanical stimulation evoked by von Frey filaments (Figure 1D) or dynamic light touch evoked by general brushing of the hind paw (Figure 1E). The withdrawal latencies to noxious cold and heat stimuli were also unaffected by the loss of lPBN neurons (Figure 1F–H). These findings suggest that, under physiological conditions, the lPBN is dispensable for driving innocuous or noxious mechanical/thermal stimulus-elicited threshold-based first-line withdrawal responses, consistent with previous research (Barik et al., 2018; Chiang et al., 2020; Han et al., 2015; Liu et al., 2022). We then assessed the second-line self-care behaviors evoked by sustained noxious stimuli, which should produce real tissue damage and pain (Huang et al., 2019). Results revealed a marked reduction in persistent licking responses induced by sustained 50°C hot plate exposure (Figure 1I), skin pinching (Figure 1J), and toe clipping (Figure 1K) in the lPBN-lesioned mice. Intraperitoneal injection of 0.6% acetic acid is widely used to assess peritoneovisceral pain (Le Bars et al., 2001; Sluka, 2013). Here, mice with lPBN neuron-ablation exhibited a 65.18% reduction in acetic acid-induced writhing responses (Figure 1L). After all behavioral tests, the IBO injection sites were examined and validated by cryosection and microscopy (Supplementary Figure S1G). These findings suggest that, under physiological conditions, lPBN neurons are required for driving sustained pain-associated recuperative rather than reflexive behaviors in response to noxious stimuli.

lPBN^{NK1R} neurons convergently relay sustained cutaneous and deep tissue pain

In our previous study, we found that spinal *Tac1*$^+$ neurons preferentially project to the slPBN and drive interoceptive responses to sustained pain (Huang et al., 2019). Furthermore, *NK1R* (also referred to as *Tacr1*)-positive neurons, which are mainly located in the slPBN, represent the major target of spinal projection (Deng et al., 2020). Thus, we suspected that lPBN^{NK1R} neurons may functionally serve as the downstream target of spinal *Tac1*$^+$ projection neurons and mediate the affective component of sustained pain. As such, we genetically labeled *NK1R*$^+$ neurons using *NK1R-CreGFP* mice (Xu et al., 2021), and characterized the co-expression of *NK1R* mRNA (Figure 2A) and NK1R protein (Supplementary Figure S2A) with the GFP reporter in the lPBN. Results indicated that most GFP$^+$ cells were co-labeled with *NK1R* mRNA (77.9%±3.4%, Figure 2A) or NK1R protein (90.1%±1.1%, Supplementary Figure S2A), and were predominantly enriched in the slPBN (76.9%±1.0% for slPBN, 20.0%±1.0% for dlPBN, Supplementary Figure S2B). Triple-color *in situ* hybridization of *NK1R* mRNA with the excitatory neuronal marker *vGlut2* and inhibitory neuronal marker *VGAT* indicated that 88.6%±1.3% of lPBN^{NK1R} neurons were excitatory, while only a small portion (6.3%±1.5%) were inhibitory (Figure 2B, C). We also used high-resolution Allen Brain Cell Atlas datasets (Yao et al., 2023) to further confirm that nearly all NK1R$^+$ neurons in the lPBN were *vGlut2*$^+$ glutamatergic neurons (Supplementary Figure S2C, D).

We examined the activation of lPBN^{NK1R} neurons in response to innocuous and noxious stimuli, and from cutaneous and deep tissues, using fiber photometry in freely moving *NK1R-CreGFP* mice injected with AAV-hSyn-DIO-GCaMP6s virus into the lPBN (Figure 2D), with the AAV-hSyn-DIO-EGFP virus used as a control (Supplementary Figure S2E–K). Results showed that innocuous mechanical stimuli, such as brush or von Frey filament application, did not increase lPBN^{NK1R} neuronal activity (Figure 2E, F; Supplementary Figure S2L, M). However, a strong increase in Ca^{2+} signals was detected when mice were exposed to a 50°C hot plate (Figure 2G), or when an alligator clip was applied to the skin or toe (Figure 2H, I). Intraperitoneal injection of acetic acid also evoked strong and long-lasting activation of lPBN^{NK1R} neurons (Figure 2J). The distribution of NK1R neurons expressing transgenic GFP reporter, and the injection sites of the GCaMP6s and EGFP control virus, were validated by cryosection and microscopy (Supplementary Figure S3). Activation of lPBN^{NK1R} neurons by noxious stimuli was further confirmed by co-staining of the c-Fos protein and GFP reporter. Results showed that 33.2%, 38.1%, and 20.9% of lPBN^{NK1R} neurons were activated by skin pinching, toe clipping, and acetic acid injection, respectively (Figure 2K–M). Thus, both intense cutaneous and deep tissue stimulation can activate lPBN^{NK1R} neurons.

Subsequently, we examined the function of lPBN^{NK1R} neurons in driving sustained pain-induced behavioral responses. Previous studies have shown that chemogenetic silencing of lPBN^{NK1R} neurons reduces second-phase licking elicited by hind paw formalin injection or paw clipping (Barik et al., 2021; Deng et al., 2020). To further clarify the function of lPBN^{NK1R} neurons, we injected AAV9-hSyn-DIO-taCasp3-TEVp virus into the lPBN of *NK1R-CreGFP* mice to selectively deplete lPBN^{NK1R} neurons (Figure 3A, B). Mice with lPBN^{NK1R} neuron-ablation exhibited behavioral phenotypes similar to those observed in whole lPBN-lesioned animals. They maintained normal sensorimotor coordination (Figure 3C) and normal reflexive withdrawal responses to external mechanical and thermal stimulation (Figure 3D–H), but a marked reduction in persistent licking behavior in response to sustained 50°C hot plate exposure, skin pinching, and toe clipping (Figure 3I–K). Similar to the whole lPBN-lesioned mice, the lPBN^{NK1R}-ablated mice showed an approximate 50% reduction in the number of writhes following intraperitoneal injection of acetic acid (Figure 3L). These findings suggest a broad involvement of lPBN neurons in inflammatory irritant-evoked peritoneovisceral pain. Given that sustained intense stimulation applied to the skin or underlying deep tissues produces pain and discomfort (Henderson et al., 2006; Huang et al., 2019; Svensson et al., 1997), we hypothesized that such intense stimuli from cutaneous and/or deep tissues should produce a strong negative teaching signal, prompting the animal to learn to avoid these stimuli. To test this, we performed skin pinching- and toe clipping-evoked CPA tests (Figure 3M). We first confirmed that sustained noxious mechanical stimuli applied on the hind paw skin or bone/muscle at the toe region induced strong aversive responses in *C57BL/6J* mice (Figure 3N). In *NK1R-CreGFP* mice, after four training sessions, the AAV-hSyn-DIO-mCherry virus-injected control group exhibited a clear aversion to the skin pinching- and toe clipping-paired compartments, whereas the lPBN^{NK1R}-ablated mice were insensitive to such

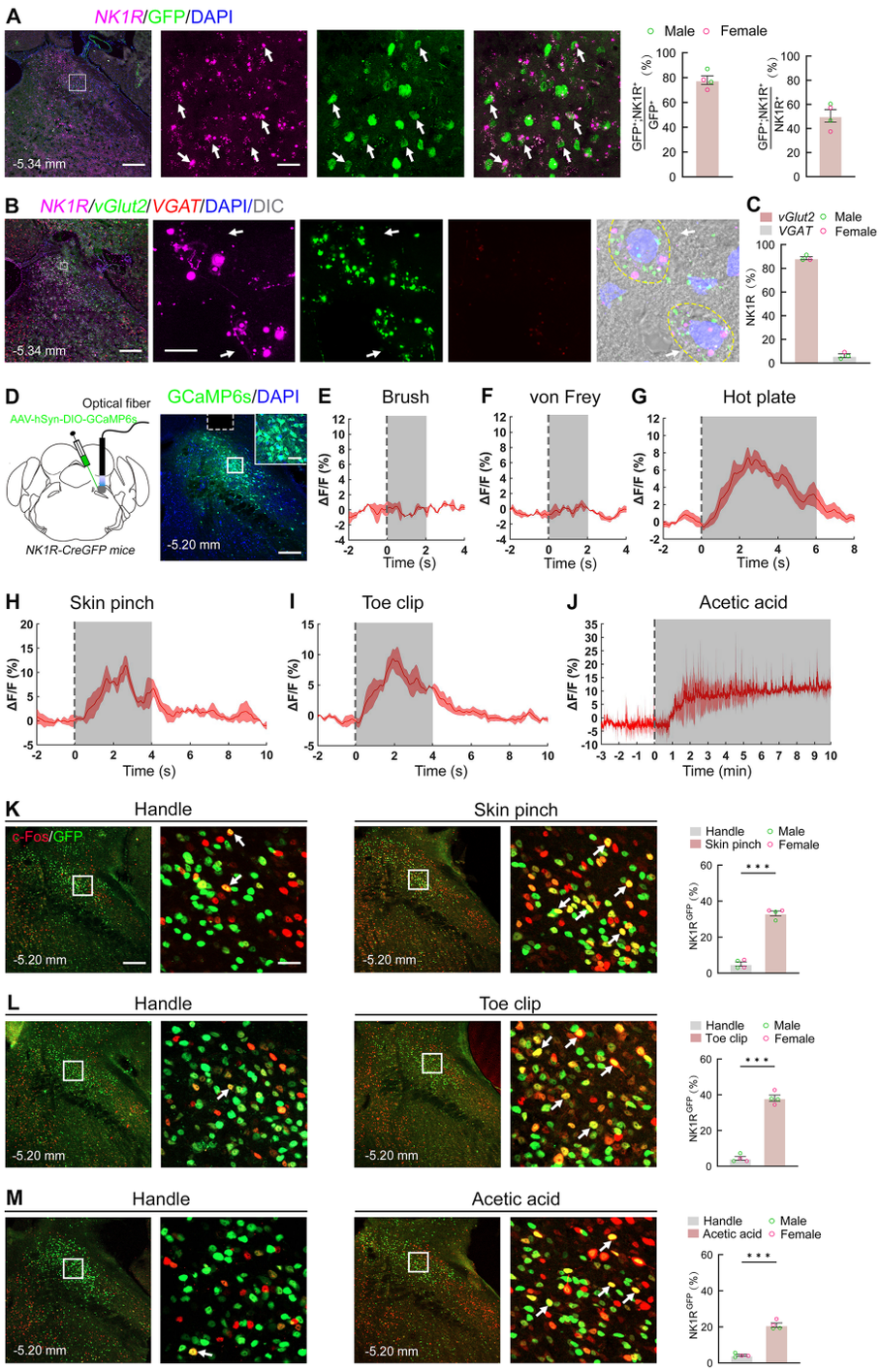

Figure 2 IPBN^{NK1R} neurons respond to sustained noxious stimuli

A: Characterization of *NK1R-CreGFP* mouse by immunostaining of GFP reporter (green) and *in situ* hybridization of *NK1R* mRNA (purple) in IPBN. Representative images show vast majority of GFP$^+$ cells are *NK1R*$^+$ (arrows). Right panels show quantification of percentage of GFP/*NK1R* co-expressing cells in GFP$^+$ or *NK1R*$^+$ populations, respectively (n=4 mice per group, including two males and two females). Scale bars: 200 μm for lower magnification and 20 μm for higher magnification, respectively. B, C: Triple-*in situ* hybridization of *NK1R* mRNA (purple) with *vGlut2* mRNA (green) and *VGAT* mRNA (red). Right panel in C shows quantification of percentage of *NK1R*$^+$ cells co-expressing *vGlut2* or *VGAT* (n=3 mice per group, including two males and one female). Scale bars: 200 μm for lower magnification and 10 μm for higher magnification. D: Left, schematic of viral injection and fiber photometry recordings for IPBN^{NK1R} neurons. Right, representative image of AAV-DIO-GCaMP6s expression in sIPBN. Scale bars: 200 μm for lower magnification and 50 μm for inset. E, F: No observed increase in average fluorescent Ca^{2+} signals in response to brush (E) and von Frey (F) stimulation (n=3 mice per test, including two males and one female). G–J: Observed increase of average fluorescent Ca^{2+} signals in response to hot plate exposure (G), skin pinching (H), toe clipping (I), and acetic acid injection (J) (n=3 mice per test, including two males and one female). K–M: Representative images of immunostaining of GFP reporter and c-Fos protein expression induced by skin pinching (K), toe clipping (L), and acetic acid injection (M). Arrows indicate co-expression of GFP and c-Fos (n=4 mice per test, including two males and two females). Scale bars: 200 μm for lower magnification, 20 μm for higher magnification, respectively. Green and red circles represent male and female mice, respectively. Data are mean±SEM, unpaired t-test. ***: P<0.001.

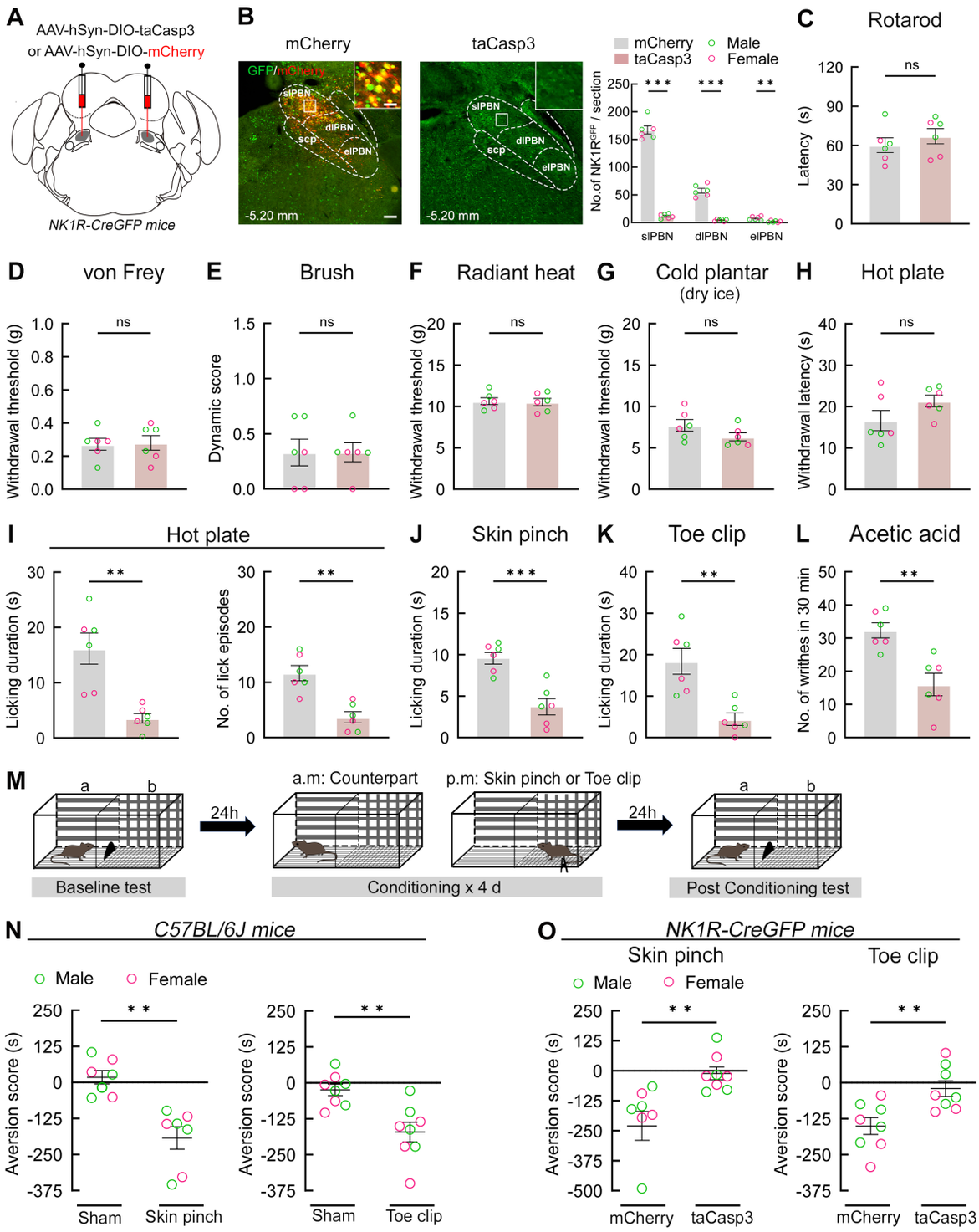

Figure 3 Depletion of lPBN^{NK1R} neurons diminish sustained pain and associated affective memory

A: Schematic of bilateral AAV viral injection to ablate lPBN^{NK1R} neurons. B: Left and middle, representative images show loss of lPBN^{NK1R} neurons (GFP, green) after taCasp3 viral injection, with mCherry as a control (red). Right, quantification of loss of GFP^{+} cells in different lPBN subnuclei after viral injection (n=6 mice per group, unpaired t-test for each lPBN subnucleus). Scale bars: 200 μm for lower magnification, 20 μm for insets. C: No significant differences were observed in falling latencies from the rotarod between control and lPBN^{NK1R}-ablated groups (n=6 mice per group). D–H: Reflexive response tests. No significant differences were observed in withdrawal responses to von Frey filament (D), brush (E), radiant heat (F), dry ice (G), and hot plate (H) stimulation (n=6–7 mice per group). I–K: lPBN^{NK1R}-ablated mice showed significantly reduced licking behaviors in hot plate (I), skin pinching (J), and toe clipping (K) tests (n=6–7 mice per group). L: Reduced writhing behavior was observed after acetic acid injection in lPBN^{NK1R}-ablated mice (n=6 mice per group). M: Schematic of skin pinching- or toe clipping-induced conditioned place aversion (CPA) test. N: Skin pinching- (left) and toe clipping-induced (right) CPA in *C57BL/6J* mice (n=7–8 mice per group). O: Both skin pinching- (left) and toe clipping-induced (right) CPA were lost in lPBN^{NK1R}-ablated mice (n=7–8 mice per group). Panels B–L, three males and three females in each group, panels N–O, four males and three to four females in each group. Green and red circles represent male and female mice, respectively. Data are mean±SEM, unpaired t-test. ns: No significance; **: P<0.01; ***: P<0.001.

conditioning (Figure 3O). Thus, lPBN^{NK1R} neurons are essential for conditioned learning and/or memory evoked by noxious stimuli that produce sustained cutaneous or deep tissue mechanical pain. To further confirm the effects of lPBN^{NK1R} neuronal ablation, we chemogenetically silenced lPBN^{NK1R} neurons. We injected AAV9-hSyn-DIO-hM4D(Gi)-mCherry and control viruses into the lPBN of *NK1R-CreGFP* mice, respectively, then measured cutaneous and deep tissue pain-associated behaviors (Supplementary Figure S4A). Before the behavioral tests, we first confirmed the silencing effect of CNO application by performing electrophysiological recordings on lPBN slices. Patch clamp recordings of hM4D(Gi)-mCherry-expressing NK1R$^+$ neurons indicated a complete loss of current injection-induced action potentials after bath application of CNO (Supplementary Figure S4B). Neuronal silencing was also confirmed by investigating skin pinch- or toe clip-induced c-Fos expression in the lPBN of mice after CNO injection (Supplementary Figure S4C). Mice with acute inhibition of lPBN^{NK1R} neurons phenocopied the lPBN^{NK1R}-ablated mice, showing a reduction in sustained cutaneous and deep tissue pain-induced recuperative behaviors, as well as normal reflexive withdrawal reactions to external nociceptive stimuli (Supplementary Figure S4D–N). The injection sites of taCasp3, hM4Di and mCherry control virus were validated by cryosection and microscopy (Supplementary Figure S5).

elPBN neurons are dispensable for driving sustained somatic thermal and mechanical pain-induced recuperative behavior

The lPBN can be divided into three major subnuclei based on their molecular and anatomical identities. Notably, elPBN neurons marked by *CGRP* serve as a general alarm to external and internal threats and are essential for producing aversive memory induced by electric foot shock and driving escape responses (Campos et al., 2018; Carter et al., 2015; Han et al., 2015; Palmiter, 2018). To further verify the function of elPBN neurons in sustained pain, we specifically ablated this lPBN subnucleus by stereotaxic microinjection of IBO into the elPBN bilaterally and confirmed neuronal loss by NeuN immunostaining (Figure 4A, B). The injection sites of IBO in the elPBN were validated by cryosection and microscopy (Supplementary Figure S6). Results showed that, under physiological conditions, loss of elPBN neurons did not affect sensorimotor coordination or withdrawal thresholds to innocuous and noxious mechanical and thermal stimuli (Figure 4C–H), consistent with previous reports (Barik et al., 2018; Chiang et al., 2020; Han et al., 2015; Liu et al., 2022). Intriguingly, although elPBN neurons serve as a general alarm, in contrast to the entire lPBN lesion, both control and elPBN-lesioned mice showed comparable amounts of licking in response to 50°C hot plate exposure, skin pinching, and toe clipping, respectively (Figure 4I–K). These observations indicated that the transmission of the affective component of sustained somatic thermal and mechanical pain was unaffected by elPBN lesion. Moreover, ablation of elPBN neurons attenuated 38.4% of the number of writhes induced by intraperitoneal acetic acid injection (Figure 4L). While elPBN neurons, such as the *CGRP*$^+$ population, play crucial roles in aversive learning and memory, elPBN lesion did not affect the CPA evoked by either skin pinching or toe clipping (Figure 4M). Thus, elPBN neurons are dispensable for driving sustained somatic thermal and mechanical pain-associated persistent licking responses and aversive learning and/or memory under physiological conditions but are involved in irritant-induced peritoneovisceral pain.

lPBN^{NK1R} neurons are dispensable for driving freezing and conditioned fear

lPBN neurons convey both affective pain and fear information to higher order brain structures (Barik et al., 2021; Campos et al., 2018; Chiang et al., 2020; Han et al., 2015; Huang et al., 2019). *CGRP*$^+$ neurons in the elPBN primarily project to the central amygdala and are required for electric foot shock-induced freezing, conditioned fear, and escape jumping from sustained hot plate exposure (Han et al., 2015). lPBN^{NK1R} neurons can also be activated by electric foot shock stimulation and hot plate exposure (Barik et al., 2021; Deng et al., 2020). However, the necessity of lPBN^{NK1R} neurons in driving fear-associated and/or escape behaviors remains unknown. Here, we observed no significant differences in freezing reactions immediately or 24 h after electric foot shock conditioning between control and lPBN^{NK1R}-ablated mice (Figure 5A, B). lPBN^{NK1R}-ablated mice also retained the jumping behavior in response to sustained 54°C hot plate exposure (Figure 5C). Consistent with previous reports (Han et al., 2015), freezing and jumping behaviors were markedly abolished in the elPBN-lesioned mice (Figure 5D–F). Thus, although lPBN^{NK1R} neurons respond to electric foot shock stimulation and noxious hot plate exposure, they are dispensable for driving fear-associated behaviors and not required for the formation of fear-associated learning and/or memory or escape behaviors. These findings strongly support the idea that lPBN neurons located in different subnuclei may drive distinct behaviors in response to pain and fear.

Taken together, our results suggest that lPBN^{NK1R} neurons are essential for driving interoceptive behaviors evoked by sustained somatic thermal and mechanical stimuli applied to cutaneous and deep tissues but are dispensable for driving freezing, conditioned fear, and escape behaviors evoked by external threats.

DISCUSSION

Understanding how the nervous system conveys multi-tissue derived noxious information and the behavioral significance of this in different animal models of pain provides fundamental guidance for pain management. The lPBN is recognized for its crucial roles in pain, fear, and visceral malaise (Buritova et al., 1998; Campos et al., 2018; Ma, 2022; Menendez et al., 1996; Palmiter, 2018; Rodella et al., 1998). However, the organizational principles of lPBN neurons in processing different types of affective information to establish negative states of the body and drive distinct behavioral outcomes remain unclear. In this study, we performed a series of pain-related behavioral assays in uninjured mice under physiological conditions and found that lPBN^{NK1R} neurons, mainly located in the slPBN, served as a convergent relay station for processing sustained cutaneous and deep tissue pain were dispensable for freezing behavior, fear-associated learning/memory, and escape behaviors to external danger. We confirmed that the elPBN is the primary driver of defensive reactions to external threats, in alignment with previous studies (Barik et al., 2018; Han et al., 2015). However, our data also indicated that elPBN neurons are dispensable for sustained somatic thermal and mechanical pain under physiological conditions.

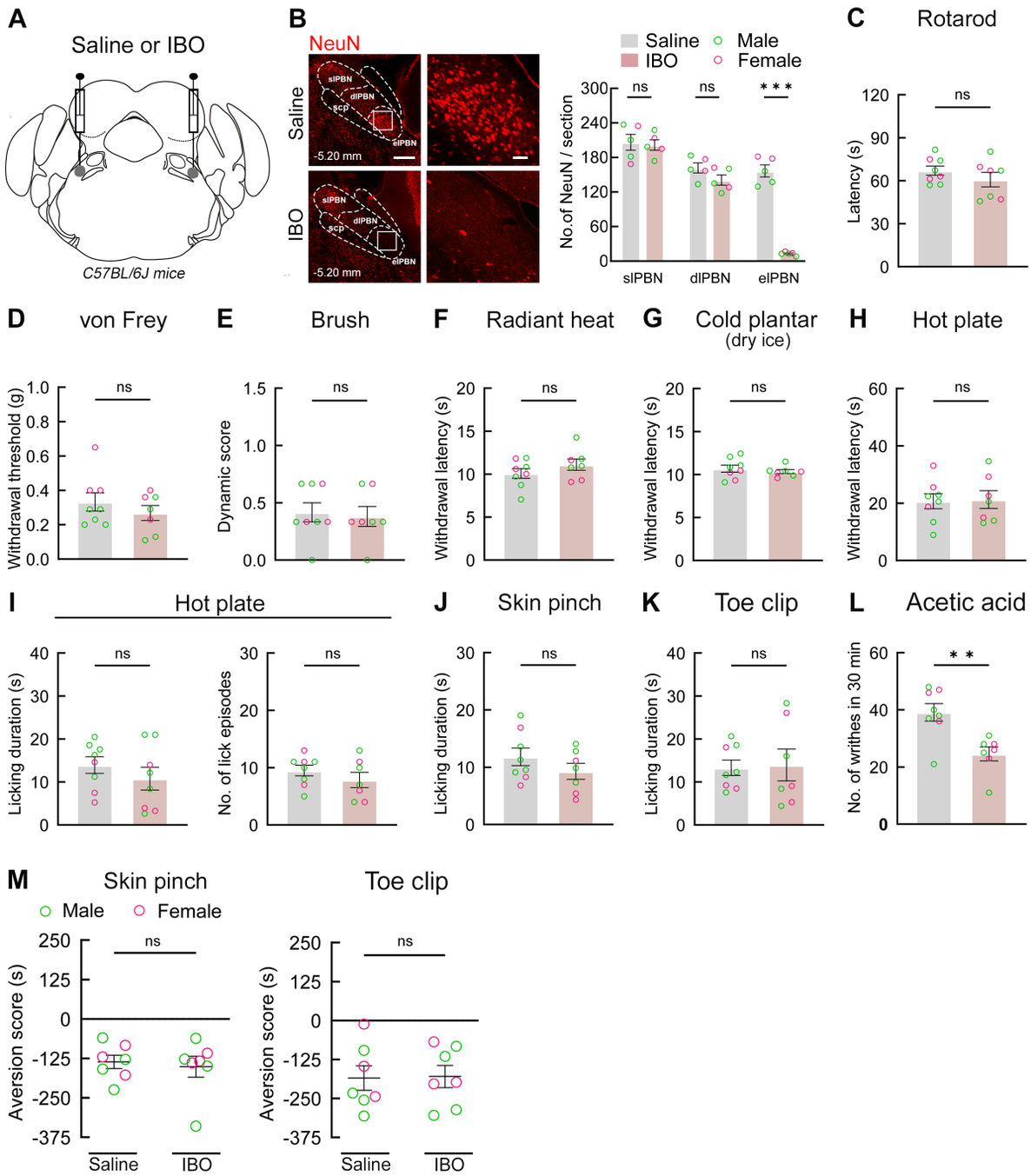

Figure 4 elPBN neurons are dispensable for sustained somatic thermal and mechanical pain

A: Schematic of elPBN specific ibotenic acid (IBO) injection. B: Left, representative immunostaining images of NeuN (red) in elPBN after saline control or IBO injection. Right, quantification of NeuN$^+$ cell number in elPBN after IBO injection (n=5 mice per group, including three males and two females). Scale bars: 200 μm for lower magnification, 20 μm for boxed higher magnification, respectively. C: No differences were observed in falling latencies from the rotarod between saline and IBO injection groups (n=7–8 mice per group). D–H: Reflexive response tests. No significant differences were observed in withdrawal responses to von Frey filament (D), brush (E), radiant heat (F), dry ice (G), and hot plate (H) stimulation (n=7–8 mice per group). I–K: elPBN-lesioned mice preserved licking behaviors in hot plate (I), skin pinching (J), and toe clipping (K) tests (n=7–8 mice per group). L: elPBN-lesioned mice (n=7–8 mice per group) showed reduced writhing behavior after acetic acid injection. M: Skin pinch- (left) or toe clip-induced (right) CPA in elPBN-lesioned mice (n=7 mice per group, including four males and three females). Panels C–L, five males and three females in saline group, four males and three females in IBO group. Green and red circles represent male and female mice, respectively. Data are mean±SEM, unpaired t-test. ns: No significance; **: P<0.01

Sensory and emotional experiences of painful stimuli are highly correlated to the origin of the stimulus (Henderson et al., 2006; Keay & Bandler, 2002; Lewis, 1942; Yang et al., 2013). lPBN neurons across all three subnuclei can be activated by noxious thermal, mechanical, and chemical stimuli applied to the skin, bone, muscle, and viscera (Buritova et al., 1998; Campos et al., 2018; Deng et al., 2020; Huang et al., 2019; Kubo et al., 2022; Lantéri-Minet et al., 1993; Palmiter, 2018; Rodella et al., 1998; Williams & Ivanusic, 2008). Our previous research showed that spinal *Tac1*$^+$

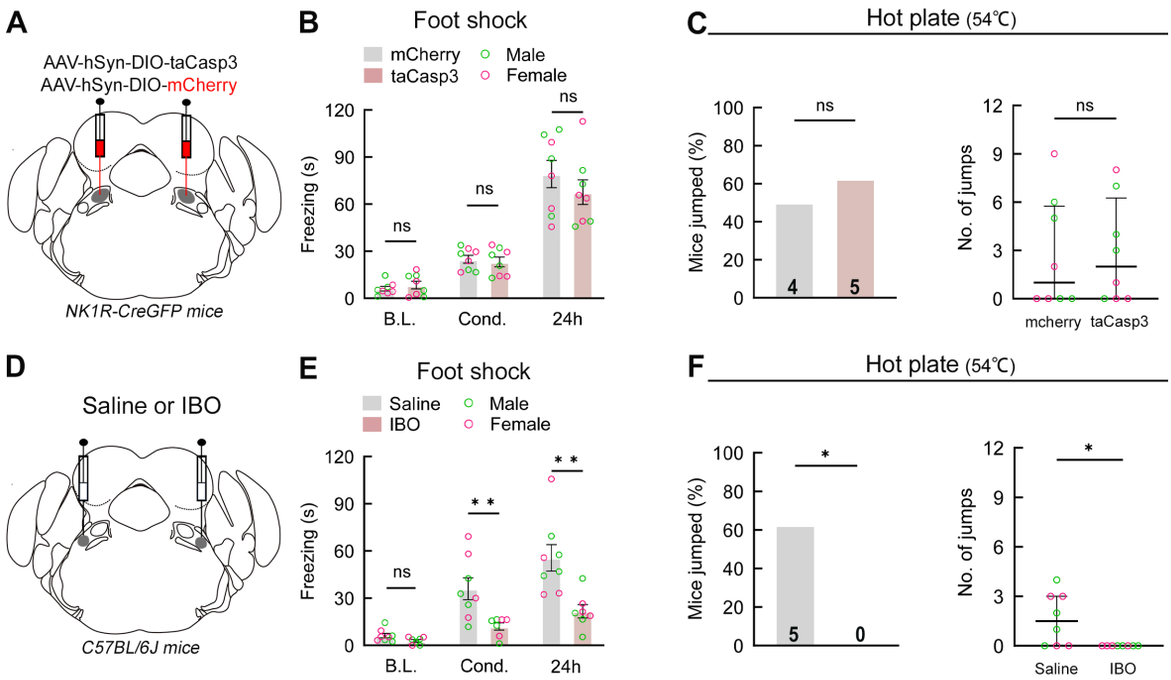

Figure 5 Functional tests of lPBN^{NK1R} and elPBN neurons in driving defensive reactions

A: Schematic of viral-based ablation of lPBN^{NK1R} neurons. B: Electric foot shock test in control and lPBN^{NK1R}-ablated mice. No significant differences were observed in freezing behavior between groups (*n*=8 mice per group, two-way ANOVA). B.L.: Baseline; Cond.: Immediately after conditioning; 24 h: 24 hours after conditioning. C: Hot plate test in control and lPBN^{NK1R}-ablated mice. No significant differences were observed in jumping behavior between groups (*n*=8 mice per group, left: Chi-square test, right: Mann-Whitney rank-sum test). Number in each bar indicates number of tested mice that jumped to escape hot plate exposure. D: Schematic of IBO injection to ablate elPBN neurons. E: Electric foot shock test in saline and IBO-injected mice. elPBN-lesioned mice showed significantly reduced freezing behavior (*n*=8 mice per group, two-way ANOVA). F: Hot plate test in saline and IBO-injected mice. elPBN-lesioned mice failed to produce jumping behavior during hot plate exposure (*n*=8 mice per group, left: Chi-square test, right: Mann-Whitney rank-sum test). Panels B, C, E, and F, four males and four females in each group. Green and red circles represent male and female mice, respectively. For Mann-Whitney rank-sum test, data are mean±quartile, others are mean±SEM. ns: No significance; *: P<0.05; **: P<0.01.

neurons, which mainly project to the slPBN, are essential for transmitting the affective component of sustained pain across different modalities (Huang et al., 2019). These behavioral phenotypes were largely replicated in the lPBN^{NK1R}-ablated mice, suggesting that lPBN^{NK1R} neurons function downstream of spinal *Tac1*$^{+}$ neurons. While research has shown that clipping the hind paw or tail can activate lPBN^{NK1R} neurons, and paw clipping-induced licking is almost abolished when lPBN^{NK1R} neurons are silenced (Barik et al., 2021), both superficial and deep somatic sensory fibers are simultaneously activated in such paradigms, making it difficult to delineate the role of lPBN^{NK1R} neurons in cutaneous and deep mechanical pain. In this study, we isolated deep tissue mechanical stimuli from the skin by topical application of lidocaine ointment and demonstrated that lPBN^{NK1R} neurons can indeed be activated by noxious mechanical input from bone/muscle in the toe region. We further showed that lPBN^{NK1R} neurons are required for both cutaneous and deep mechanical stimulation-induced persistent licking behavior and CPA. Interestingly, although elPBN neurons (mostly *CGRP*$^{+}$) respond to a wide range of somatic and visceral sensory inputs, and serve as a general alarm (Campos et al., 2018; Han et al., 2015; Palmiter, 2018), mice with elPBN lesions retained persistent licking behavior when exposed to sustained hot plate and mechanical stimuli applied to the skin and toe. Furthermore, the elPBN-ablated mice showed comparable levels of skin pinch- or toe clip-induced CPA as the control mice. This may be explained by the fact that pharmacogenetic or optogenetic activation of lPBN^{NK1R} neurons is sufficient to generate spontaneous licking behavior and pain affects (Deng et al., 2020). Therefore, under physiological conditions, slPBN *NK1R*$^{+}$ neurons, rather than elPBN neurons, dominate in processing the affective dimension of sustained somatic thermal and mechanical pain and are required for driving interoceptive responses and aversive memory induced by such painful stimulation.

Irritants such as acetic acid or bradykinin injected into the peritoneum activate neurons throughout the lPBN and induce peritoneovisceral pain, as indicated by stereotyped writhing behavior (Bernard et al., 1994; Lantéri-Minet et al., 1993; Le Bars et al., 2001). We confirmed that writhing behavior was significantly attenuated in lPBN-lesioned mice, while the remaining peritoneovisceral nocifensive responses may be driven by direct spinal cord projections to the medial thalamic complex (Ren et al., 2009; Wang et al., 2007). However, in contrast to the clear functional segregation of slPBN and elPBN neurons in processing sustained somatic thermal and mechanical pain, both the lPBN^{NK1R}-ablated and elPBN-lesioned mice showed a significant reduction in writhing after intraperitoneal injection of acetic acid. These findings are consistent with the observation that pharmacogenetic suppression of either lPBN^{NK1R} neurons or *Oprm1*$^{+}$ neurons in the elPBN attenuate hind paw formalin injection-induced licking behavior (Deng et al., 2020; Liu et al., 2022). Thus, slPBN and elPBN neurons, along with potentially dlPBN neurons, are broadly involved in driving chemical or

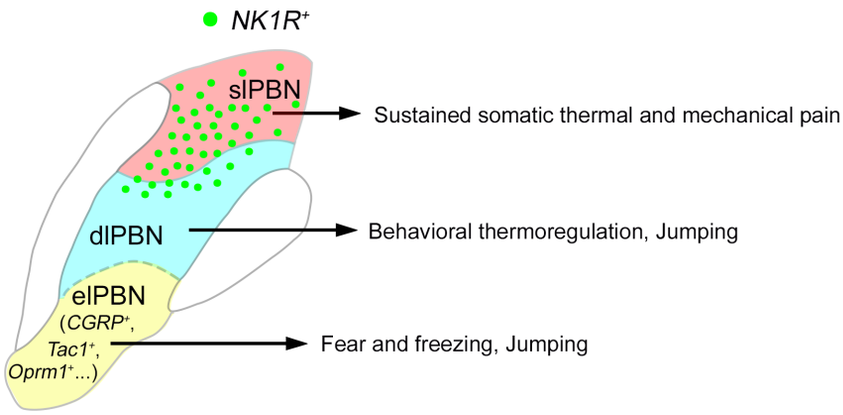

Note: All three lPBN subnuclei may contribute to the nocifensive and emotional responses induced by sustained infammatory irritation.

Figure 6 Functional requirement of lPBN neurons for driving distinct behaviors in response to noxious stimuli

Summary of roles of neurons in different lPBN subnuclei for driving distinct behaviors in responses to noxious stimuli under physiological conditions. As a whole population, *NK1R*$^{+}$ neurons (green dots), mainly located in the slPBN, are required for driving persistent licking induced by sustained noxious thermal and mechanical stimuli applied to the skin and bone/muscle. dlPBN neurons are required for behavioral thermoregulation (Yahiro et al., 2017), and are also involved in provoking jumping behavior (Chiang et al., 2020). elPBN neurons (mainly expressing *CGRP*, *Tac1*, or *Oprm1*) are required for driving defensive reactions such as freezing and jumping, as well as conditioned fear (Barik et al., 2018; Han et al., 2015; Liu et al., 2022 and this study). Both elPBN and slPBN (and potentially dlPBN) neurons are required for inducing nocifensive and emotional responses after inflammatory irritation, such as hind paw formalin injection or intraperitoneal injection of acetic acid (Deng et al., 2020; Liu et al., 2020; This study).

inflammatory irritation-evoked sustained somatic and peritoneovisceral pain.

The scope of current study aimed to dissect the function of lPBN neurons located in different subnuclei in transmitting nociceptive information under physiological conditions. Consistent with previous studies (Barik et al., 2018; Chiang et al., 2020; Han et al., 2015; Liu et al., 2022), our findings confirmed that loss of lPBN neurons, lPBN^{NK1R} neurons, or elPBN neurons does not affect baseline reflexive responses to peripheral mechanical and thermal stimuli. A quick withdrawal reflex from noxious stimulation can be mediated by segmental spinal circuits in the absence of supraspinal activation (Cobos & Portillo-Salido, 2013; Sluka, 2013; Woolf & Swett, 1984). However, inhibition of lPBN neurons reverses CFA injection-induced mechanical hypersensitivity (Chiang et al., 2020). A recent study indicated that inhibition of central amygdala-projecting lPBN neurons attenuates nerve injury-induced mechanical and thermal hypersensitivity without affecting baseline nociception (Torres-Rodriguez et al., 2024). Moreover, a contralateral brain-to-spinal cord descending pathway, starting from lPBN *Oprm1*$^{+}$ neurons, acts to prevent the induction of contralateral mechanical allodynia following nerve injury (Huo et al., 2023). Thus, under pathological conditions, lPBN neurons indeed play important roles in modulating sensitized reflexive behaviors.

Taken together, our work revealed the functional organization of lPBN neurons in driving sustained pain, fear, and escape behaviors under physiological conditions. Our findings identified a functional segregation of lPBN neurons in producing distinct behaviors in response to sustained somatic thermal and mechanical pain versus external threats (Figure 6). As writhing behavior may contain a mixture of reflexive and affective components (Hammond, 1989; Le Bars et al., 2001), the detailed roles of lPBN neurons in transmitting acetic acid-induced peritoneovisceral pain warrant further investigation.

SUPPLEMENTARY DATA

Supplementary data to this article can be found online.

COMPETING INTERESTS

The authors declare that they have no competing interests.

AUTHORS' CONTRIBUTIONS

J.D.X., Y.J.Z., and T.W.H. designed the experiments. J.K., W.C.L., H.Y.J., S.Q., S.W.M., G.F.C., W.X.Q., X.J.C., Q.Z., S.S.L., and L.Z. performed the experiments and analyzed the data. J.K., W.C.L., H.Y.J., and T.W.H. wrote the manuscript. J.D.X., Y.J.Z., and T.W.H. revised the manuscript and supported all aspects of this study. All authors read and approved the final version of the manuscript.

ACKNOWLEDGMENTS

We thank Dr. Xin-Zhong Dong for providing *NK1R-CreGFP* mice. We would like to express our sincere gratitude to Dr. Qiu-Fu Ma (Westlake University), Dr. Feng Wang (Shenzhen Institute of Advanced Technology, Chinese Academy of Sciences), and Dr. Long-Zhen Cheng (Southern University of Science and Technology) for their helpful comments and kind suggestions on the manuscript.

REFERENCES

Barik A, Sathyamurthy A, Thompson J, et al. 2021. A spinoparabrachial circuit defined by Tacr1 expression drives pain. *eLife*, **10**: e61135.

Barik A, Thompson JH, Seltzer M, et al. 2018. A brainstem-spinal circuit controlling nocifensive behavior. *Neuron*, **100**(6): 1491–1503. e3.

Basbaum AI, Bautista DM, Scherrer G, et al. 2009. Cellular and molecular mechanisms of pain. *Cell*, **139**(2): 267–284.

Beecher HK. 1957. The measurement of pain; prototype for the quantitative study of subjective responses. *Pharmacological Reviews*, **9**(1): 59–209.

Bernard JF, Huang GF, Besson JM. 1994. The parabrachial area: electrophysiological evidence for an involvement in visceral nociceptive processes. *Journal of Neurophysiology*, **71**(5): 1646–1660.

Bourane S, Grossmann KS, Britz O, et al. 2015. Identification of a spinal circuit for light touch and fine motor control. *Cell*, **160**(3): 503–515.

Brenner DS, Golden JP, Gereau IV RW. 2012. A novel behavioral assay for measuring cold sensation in mice. *PLoS One*, **7**(6): e39765.

Buritova J, Besson JM, Bernard JF. 1998. Involvement of the spinoparabrachial pathway in inflammatory nociceptive processes: a c-Fos protein study in the awake rat. *Journal of Comparative Neurology*, **397**(1):

10–28.
Campos CA, Bowen AJ, Roman CW, et al. 2018. Encoding of danger by parabrachial CGRP neurons. *Nature*, **555**(7698): 617–622.
Carter ME, Han S, Palmiter RD. 2015. Parabrachial calcitonin gene-related peptide neurons mediate conditioned taste aversion. *Journal of Neuroscience*, **35**(11): 4582–4586.
Chaplan SR, Bach FW, Pogrel JW, et al. 1994. Quantitative assessment of tactile allodynia in the rat paw. *Journal of Neuroscience Methods*, **53**(1): 55–63.
Chen WG, Schloesser D, Arensdorf AM, et al. 2021. The emerging science of interoception: sensing, integrating, interpreting, and regulating signals within the self. *Trends in Neurosciences*, **44**(1): 3–16.
Cheng LZ, Duan B, Huang TW, et al. 2017. Identification of spinal circuits involved in touch-evoked dynamic mechanical pain. *Nature Neuroscience*, **20**(6): 804–814.
Chiang MC, Bowen A, Schier LA, et al. 2019. Parabrachial complex: a hub for pain and aversion. *Journal of Neuroscience*, **39**(42): 8225–8230.
Chiang MC, Nguyen EK, Canto-Bustos M, et al. 2020. Divergent neural pathways emanating from the lateral parabrachial nucleus mediate distinct components of the pain response. *Neuron*, **106**(6): 927–939. e5.
Choi S, Hachisuka J, Brett MA, et al. 2020. Parallel ascending spinal pathways for affective touch and pain. *Nature*, **587**(7833): 258–263.
Cobos EJ, Portillo-Salido E. 2013. "Bedside-to-bench" behavioral outcomes in animal models of pain: beyond the evaluation of reflexes. *Current Neuropharmacology*, **11**(6): 560–591.
Deng J, Zhou H, Lin JK, et al. 2020. The parabrachial nucleus directly channels spinal nociceptive signals to the intralaminar thalamic nuclei, but not the amygdala. *Neuron*, **107**(5): 909–923. e6.
Duan B, Cheng LZ, Bourane S, et al. 2014. Identification of spinal circuits transmitting and gating mechanical pain. *Cell*, **159**(6): 1417–1432.
Fulwiler CE, Saper CB. 1984. Subnuclear organization of the efferent connections of the parabrachial nucleus in the rat. *Brain Research Reviews*, **7**(3): 229–259.
Gauriau C, Bernard JF. 2002. Pain pathways and parabrachial circuits in the rat. *Experimental Physiology*, **87**(2): 251–258.
Hammond DL. 1989. Inference of pain and its modulation from simple behaviors. *In*: Chapman CR, Loeser JD. Issues in Pain Measurement: Advances in Pain Research and Therapy. New York: Raven, 69–91.
Han S, Soleiman MT, Soden ME, et al. 2015. Elucidating an affective pain circuit that creates a threat memory. *Cell*, **162**(2): 363–374.
Han ZP, Luo NS, Ma WY, et al. 2023. AAV11 enables efficient retrograde targeting of projection neurons and enhances astrocyte-directed transduction. *Nature Communications*, **14**(1): 3792.
Hargreaves K, Dubner R, Brown F, et al. 1988. A new and sensitive method for measuring thermal nociception in cutaneous hyperalgesia. *Pain*, **32**(1): 77–88.
Hashimoto K, Obata K, Ogawa H. 2009. Characterization of parabrachial subnuclei in mice with regard to salt tastants: possible independence of taste relay from visceral processing. *Chemical Senses*, **34**(3): 253–267.
Head H. 1911. Sensory disturbances from cerebral lesions. *Brain*, **34**(2-3): 102–254.
Henderson LA, Bandler R, Gandevia SC, et al. 2006. Distinct forebrain activity patterns during deep versus superficial pain. *Pain*, **120**(3): 286–296.
Hou GQ, Jiang SL, Chen GW, et al. 2023. Opioid receptors modulate firing and synaptic transmission in the paraventricular nucleus of the thalamus. *Journal of Neuroscience*, **43**(15): 2682–2695.
Hu ZF, Mu YM, Huang L, et al. 2022. A visual circuit related to the periaqueductal gray area for the antinociceptive effects of bright light treatment. *Neuron*, **110**(10): 1712–1727. e7.
Huang DK, Grady FS, Peltekian L, et al. 2021a. Efferent projections of Vglut2, Foxp2, and Pdyn parabrachial neurons in mice. *Journal of Comparative Neurology*, **529**(4): 657–693.
Huang DK, Grady FS, Peltekian L, et al. 2021b. Efferent projections of CGRP/*Calca*-expressing parabrachial neurons in mice. *Journal of Comparative Neurology*, **529**(11): 2911–2957.
Huang TW, Lin SH, Malewicz NM, et al. 2019. Identifying the pathways required for coping behaviours associated with sustained pain. *Nature*, **565**(7737): 86–90.
Huo JT, Du F, Duan KF, et al. 2023. Identification of brain-to-spinal circuits controlling the laterality and duration of mechanical allodynia in mice. *Cell Reports*, **42**(4): 112300.
Jaramillo AA, Brown JA, Winder DG. 2021. Danger and distress: parabrachial-extended amygdala circuits. *Neuropharmacology*, **198**: 108757.
Keay KA, Bandler R. 2002. Distinct central representations of inescapable and escapable pain: observations and speculation. *Experimental Physiology*, **87**(2): 275–279.
Kim SY, Adhikari A, Lee SY, et al. 2013. Diverging neural pathways assemble a behavioural state from separable features in anxiety. *Nature*, **496**(7444): 219–223.
Kubo A, Sugawara S, Iwata K, et al. 2022. Masseter muscle contraction and cervical muscle sensitization by nerve growth factor cause mechanical hyperalgesia in masticatory muscle with activation of the trigemino-lateral parabrachial nucleus system in female rats. *Headache: the Journal of Head and Face Pain*, **62**(10): 1365–1375.
Lantéri-Minet M, Isnardon P, De Pommery J, et al. 1993. Spinal and hindbrain structures involved in visceroception and visceronociception as revealed by the expression of Fos, Jun and Krox-24 proteins. *Neuroscience*, **55**(3): 737–753.
Le Bars D, Gozariu M, Cadden SW. 2001. Animal models of nociception. *Pharmacological Reviews*, **53**(4): 597–652.
Lewis T. 1942. Pain. New York: McMillan.
Liu SJ, Ye M, Pao GM, et al. 2022. Divergent brainstem opioidergic pathways that coordinate breathing with pain and emotions. *Neuron*, **110**(5): 857–873. e9.
Lou S, Duan B, Vong L, et al. 2013. Runx1 controls terminal morphology and mechanosensitivity of VGLUT3-expressing C-mechanoreceptors. *Journal of Neuroscience*, **33**(3): 870–882.
Ma QF. 2022. A functional subdivision within the somatosensory system and its implications for pain research. *Neuron*, **110**(5): 749–769.
Mao JR. 2012. Current challenges in translational pain research. *Trends in Pharmacological Sciences*, **33**(11): 568–573.
Mark VH, Ervin FR, Hackett TP. 1960. Clinical aspects of stereotactic thalamotomy in the human. Part I. The treatment of chronic severe pain. *Archives of Neurology*, **3**: 351–367.
Mark VH, Ervin FR, Yakovlev PI. 1963. Stereotactic thalamotomy III. The verification of anatomical lesion sites in the human thalamus. *Archives of Neurology*, **8**(5): 528–538.
Menendez L, Bester H, Besson JM, et al. 1996. Parabrachial area: electrophysiological evidence for an involvement in cold nociception. *Journal of Neurophysiology*, **75**(5): 2099–2116.
Mogil JS. 2009. Animal models of pain: Progress and challenges. *Nature Reviews Neuroscience*, **10**(4): 283–294.
Mogil JS. 2018. Friends in pain: pain tolerance in a social network. *Scandinavian Journal of Pain*, **18**(3): 343–344.
Palmiter RD. 2018. The parabrachial nucleus: CGRP neurons function as a general alarm. *Trends in Neurosciences*, **41**(5): 280–293.
Pauli JL, Chen JY, Basiri ML, et al. 2022. Molecular and anatomical characterization of parabrachial neurons and their axonal projections. *eLife*, **11**: e81868.
Paxinos G, Franklin KBJ. 2013. Paxinos and Franklin's the Mouse Brain in Stereotaxic Coordinates. 4th ed. Amsterdam: Elsevier.

Ren Y, Zhang LP, Lu Y, et al. 2009. Central lateral thalamic neurons receive noxious visceral mechanical and chemical input in rats. *Journal of Neurophysiology*, **102**(1): 244–258.

Rodella L, Rezzani R, Gioia M, et al. 1998. Expression of Fos immunoreactivity in the rat supraspinal regions following noxious visceral stimulation. *Brain Research Bulletin*, **47**(4): 357–366.

Roeder Z, Chen QL, Davis S, et al. 2016. Parabrachial complex links pain transmission to descending pain modulation. *Pain*, **157**(12): 2697–2708.

Saper CB. 2016. The house alarm. *Cell Metabolism*, **23**(5): 754–755.

Sluka KA. 2013. Ask the Experts: peripheral and central mechanisms of chronic musculoskeletal pain. *Pain Management*, **3**(2): 103–107.

Sun L, Liu R, Guo F, et al. 2020. Parabrachial nucleus circuit governs neuropathic pain-like behavior. *Nature Communications*, **11**(1): 5974.

Svensson P, Minoshima S, Beydoun A, et al. 1997. Cerebral processing of acute skin and muscle pain in humans. *Journal of Neurophysiology*, **78**(1): 450–460.

Tappe-Theodor A, King T, Morgan MM. 2019. Pros and cons of clinically relevant methods to assess pain in rodents. *Neuroscience & Biobehavioral Reviews*, **100**: 335–343.

Torres-Rodriguez JM, Wilson TD, Singh S, et al. 2024. The parabrachial to central amygdala pathway is critical to injury-induced pain sensitization in mice. *Neuropsychopharmacology*, **49**(3): 508–520.

Tovote P, Fadok JP, Lüthi A. 2015. Neuronal circuits for fear and anxiety. *Nature Reviews Neuroscience*, **16**(6): 317–331.

Wang HC, Chia SC, Wu YS, et al. 2007. Does the medial thalamus play a role in the negative affective component of visceral pain in rats. *Neuroscience Letters*, **420**(1): 80–84.

Williams MC, Ivanusic JJ. 2008. Evidence for the involvement of the spinoparabrachial pathway, but not the spinothalamic tract or post-synaptic dorsal column, in acute bone nociception. *Neuroscience Letters*, **443**(3): 246–250.

Woolf CJ, Swett JE. 1984. The cutaneous contribution to the hamstring flexor reflex in the rat: an electrophysiological and anatomical study. *Brain Research*, **303**(2): 299–312.

Xu Q, Ford NC, He SQ, et al. 2021. Astrocytes contribute to pain gating in the spinal cord. *Science Advances*, **7**(45): eabi6287.

Yahiro T, Kataoka N, Nakamura Y, et al. 2017. The lateral parabrachial nucleus, but not the thalamus, mediates thermosensory pathways for behavioural thermoregulation. *Scientific Reports*, **7**(1): 5031.

Yang FC, Tan T, Huang TW, et al. 2013. Genetic control of the segregation of pain-related sensory neurons innervating the cutaneous versus deep tissues. *Cell Reports*, **5**(5): 1353–1364.

Yao ZZ, van Velthoven CTJ, Kunst M, et al. 2023. A high-resolution transcriptomic and spatial atlas of cell types in the whole mouse brain. *Nature*, **624**(7991): 317–332.

Zylka MJ, Rice FL, Anderson DJ. 2005. Topographically distinct epidermal nociceptive circuits revealed by axonal tracers targeted to *Mrgprd*. *Neuron*, **45**(1): 17–25.